1521-009X/50/2/95–104$35.00
DRUG METABOLISM AND DISPOSITION
dx.doi.org/10.1124/dmd.121.000552
Drug Metab Dispos 50:95–104, February 2022

DRUG METABOLISM & DISPOSITION

Evaluation of ADMET Predictor in Early Discovery Drug Metabolism and Pharmacokinetics Project Work

Anna-Karin Sohlenius-Sternbeck and Ylva Terelius

Research Institutes of Sweden, Södertälje, Sweden (A.-K.S.-S.); ADMEYT AB, Stenhamra, Sweden (Y.T.); and Medivir AB, Huddinge, Sweden (A.-K.S.-S., Y.T.)

Received May 25, 2021; accepted November 5, 2021

ABSTRACT

A dataset consisting of measured values for LogD, solubility, metabolic stability in human liver microsomes (HLMs), and Caco-2 permeability was used to evaluate the prediction models for lipophilicity (S+LogD), water solubility (S+Sw_pH), metabolic stability in HLM (CYP_HLM_Clint), intestinal permeability (S+P_{eff}), and P-glycoprotein (P-gp) substrate identification (P-gp substrate) in the software ADMET Predictor (AP) from Simulations Plus. The dataset consisted of a total of 4,794 compounds, with at least data from metabolic stability determinations in HLM, from multiple discovery projects at Medivir. Our evaluation shows that the global AP models can be used for categorization of high and low values based on predicted results for metabolic stability in HLM and intestinal permeability, and to give good predictions of LogD (R^2 = 0.79), guiding the synthesis of new compounds and for prioritizing in vitro ADME experiments. The model seems to overpredict solubility for the Medivir compounds, however. We also used the in-house datasets to build local models for LogD, solubility, metabolic stability, and permeability by using artificial neural network (ANN) models in the optional Modeler module of AP. Predictions of the test sets were performed with both the global and the local models, and the R^2 values for linear regression for predicted versus measured HLM in vitro intrinsic clearance (CL_{int}) based on logarithmic data were 0.72 for the in-house model and 0.53 for the AP model. The improved predictions with the local models are likely explained both by the specific chemical space of the Medivir dataset and laboratory-specific assay conditions for parameters that require biologic assay systems.

SIGNIFICANCE STATEMENT

AP is useful early in projects for predicting and categorizing LogD, metabolic stability, and permeability, to guide the synthesis of new compounds, and for prioritizing in vitro ADME experiments. The building of local in-house prediction models with the optional AP Modeler Module can yield improved prediction success since these models are built on data from the same experimental setup and can also be based on compounds with similar structures.

Introduction

In vivo drug disposition is dependent on the interactions between the drug and the body. During the drug discovery phase, chemical synthesis is guided toward potent compounds with physicochemical and absorption, distribution, metabolism, and excretion (ADME) properties that allow the drug to reach effective concentrations at the target (Ballard et al., 2012; Sohlenius-Sternbeck et al., 2016). Also, compounds should show low toxicity (Kramer et al., 2007). Early characterization and understanding of the properties of new chemical entities facilitate the further optimization of a chemical series toward a new drug candidate.

Reliable in silico prediction tools for ADME properties can help decision making in the early phase of drug discovery, even before experimental data are available (van de Waterbeemd, 2003; Moda et al., 2008; Wang et al., 2015; Alqahtani, 2017; Kazmi et al., 2018; Stålring et al., 2018). With such tools, the chemical design and synthesis can be prioritized and focus on compounds with the best potential to show desired properties later in vivo. The building of quantitative structure–activity/quantitative structure–property relationships (QSAR/QSPR) models is highly dependent on the quality of the training set data (Gleeson and Montanari, 2012). Moreover, metabolism, distribution and excretion involve multi-mechanistic processes which make the building of in silico models challenging.

The use of a commercial software for predictions of chemical and ADMET properties is convenient, since such tools can be used with virtual compounds and do not require any user data while measured data are needed for local model building. However, in the commercial models, the chemical space of the local compounds may not be covered. It is also likely that commercial models are built on datasets from multiple sources with dissimilarities in the experimental setup. For many assays, the experimental variability between different laboratories is substantial (Hayeshi, 2008; Liu, 2015), which often makes it desirable to build in-house local models. A local model would also better cover the chemical space of in-house compounds, especially within a project/project series with similar structures, and the user can have control over the training set. However, when building in-house models, a large enough training

This work received no external funding.
No author has an actual or perceived conflict of interest with the contents of this manuscript.
dx.doi.org/10.1124/dmd.121.000552.

ABBREVIATIONS: ABBA, apical to basolateral and basolateral to apical; ADME, absorption, distribution, metabolism, excretion; ANN, artificial neural network; AP, ADMET Predictor; CL_{int}, in vitro intrinsic clearance; GF, GF120918 (Elacridar); HLM, human liver microsomes; HPLC, high-performance liquid chromatography; MAE, mean absolute error; P_{app}, apparent permeability; P_{eff}, effective jejunal permeability; P-gp, P-glycoprotein; QSAR, quantitative structure–activity relationship; QSPR, quantitative structure–property relationship; RMSE, root mean square error.

set with good quality data covering the chemical space is needed. For these reasons, large pharmaceutical companies have their own dedicated modelers responsible for building in-house project-specific QSAR/QSPR models.

Several commercial software types or online prediction tools are available for ADME, pharmacokinetic, pharmacokinetic–pharmacodynamic, DDI (drug–drug interactions), and toxicity predictions. We have previously successfully used GastroPlus from Simulations Plus, Inc., as part of a strategy to identify risks for DDI in drug discovery (Sohlenius-Sternbeck et al., 2018). ADMET Predictor (AP) from Simulations Plus, Inc. is a commercially available software for prediction of physical chemistry, ADME and toxicity parameters from compound structures.

In this work, we used a dataset with experimental in-house data to evaluate whether the global models in the commercially available AP software can be used as tools in early drug discovery (before in-house data are available). The parameters predicted were water solubility, lipophilicity, metabolic stability in human liver microsomes (HLM), permeability and whether a compound will be a substrate for P-glycoprotein (P-gp). Included in the study were 4794 compounds in the Medivir database with metabolic stability data in HLM. The dataset consists of compounds from multiple discovery projects at Medivir, and it comprises mainly protease inhibitors and nucleoside analogs, which may not be well represented in the training set for the global models. We evaluated the AP models for LogD (S+LogD), water solubility (S+S_pH), metabolic stability in HLM (CYP_HLM_Clint), permeability (S+P_{eff}), and P-gp substrate (Yes/No) by comparing predicted values with experimental results.

The ADMET Modeler tool is an optional module in AP and can be used to build local and/or project specific models based on QSAR/QSPR and by using chemical descriptors obtained with the AP software. The module is licensed separately and can be used without extensive knowledge in modeling. With the ADMET Modeler Module, local ANN models for Log D, solubility, metabolic stability and permeability were built using the Medivir dataset, and the models were tested on in-house compounds as well as on commercially available reference compounds. The outcome of the local in-house models was compared with the outcome of the global AP models. A good training set is required for a predictive outcome, and the larger and the more similar the structures in the training set the better the predictive outcome, but we have previously built local models for projects in lead optimization phase based on training sets of about 20 similar compounds from a single compound series. These were useful and predictive for the next round of synthesis but had to be rebuilt often as the results were used to improve the structures, moving away from the training set structures (unpublished results).

Materials and Methods

Chemicals. All chemicals were of analytical grade and obtained from commercial suppliers.

Characteristics of the Medivir Dataset. The vast majority of the compounds in the Medivir dataset had a purity ≥95% according to high-performance liquid chromatography (HPLC) analysis (no compound had a purity ≤80%). Compounds observed to be chemically unstable or poorly soluble during the experiments were removed (i.e., 78 compounds). The distribution of molecular weight (of the remaining 4794 compounds) and measured LogD (1198 compounds) for the Medivir compounds are shown in Figs. 1A and B, respectively. There were 2236 zwitterions, 1888 bases, 623 acids, 44 neutrals, and 3 compounds with mixed pKa values in the dataset. Most of the acids were weak with pKa values above 7 (only 52 acids had a pKa below 5). Also, most of the bases were weak bases with pKa below 7 (only 385 bases had a pKa above 8).

Predictions of ADME Properties. Predictions of ADME properties were made using the ADMET Predictor software, here called AP (version 9.5,

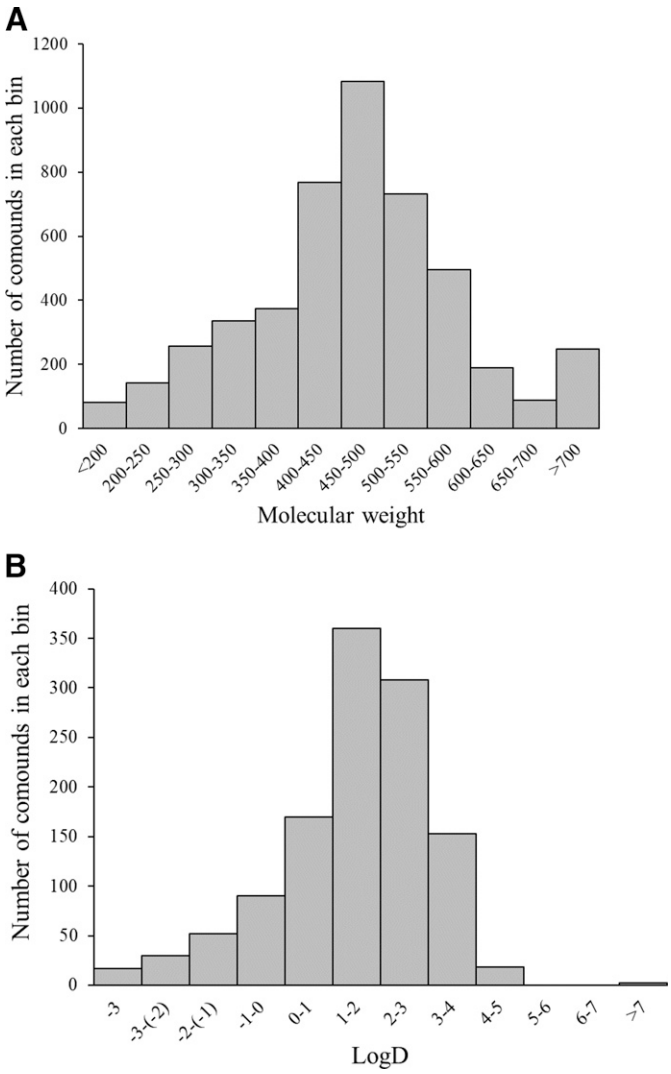

Fig. 1. Characteristics of the Medivir dataset (4794 compounds) demonstrated by histograms showing (A) the distribution of molecular weight and (B) the distribution of measured LogD (1198 compounds).

Simulations Plus, Inc., Lancaster, CA; http://www.simulations-plus.com), and the chemical structures were defined by the simplified molecular-input line-entry system. The software models for LogD (S+LogD), water solubility (S+Sw_pH, i.e., solubility at a certain chosen pH, here pH 7.4), metabolic stability (CYP_HLM_Clint), effective jejunal permeability (S+P_{eff}), and P-gp substrate identification were evaluated using the Medivir dataset.

Moreover, in-house local models were built on training sets from the Medivir dataset, using artificial neural network ensembles in the optional ADMET Modeler module (Modeler). The Modeler uses an early stopping technique, in which the interplay between the model complexity and quality of output are taken into account to avoid the generation of an overtrained model. The in-house models for solubility, HLM CL_{int}, and Caco-2 permeability were based on logarithmic data. A training set that represented approximately 75–80% of the measured values was used for each parameter, and the remaining 20–25% was used as a test set to evaluate the model. The test sets were selected in the ADMET Modeler module based on Kohonen mapping (Yan and Gasteiger, 2003). The test sets were also evaluated in the corresponding ADMET Predictor software global models. Each model was rebuilt at least four times, and the deviation for each statistical parameter (see the statistical section) was around 10% or less between the models. Tables and figures show data from one representative model for each assay.

Determination of LogD. Determination of LogD was performed for Medivir by GVK Biosciences Limited (Hyderabad, India). LogD was determined by

measuring the partition coefficient between water and octanol at pH 7.4. Fifteen microliters of test compound stock solution (10 mM in DMSO) was added to 500 μl of octanol in 3 replicates and vortexed for 10 minutes on a plate shaker at 1200 rpm. Five hundred microliters of 10 mM phosphate buffer, pH 7.4, was added, and the mixture was vortexed for another hour at 1200 rpm. The samples were allowed to settle for 20 minutes and then centrifuged at 4000 rpm for 30 minutes at room temperature for complete phase separation and analyzed by HPLC-UV absorbance.

Determination of Kinetic Solubility. Kinetic solubility measurements were also performed at GVK Biosciences Limited (Hyderabad, India). A stock solution of 10 mM compound in DMSO was added to 10 mM phosphate buffered saline, pH 7.4, to give a final compound concentration of 100 μM in 10 mM phosphate with 1% DMSO. After a period of vigorous vortexing, the precipitate was removed by vacuum filtration. No correction for non-specific binding was performed. The compound concentration in the resulting filtrate was determined by HPLC-UV absorbance. The kinetic solubility assay could not generate solubilities above 100 μM since that was the final concentration added in the assay. Thus, higher solubilities were reported as >100 μM.

Determination of Permeability. Permeability in Caco-2 cells (Artursson et al., 2001) was assayed at Medivir or at GVK Biosciences Limited (Hyderabad, India) using the same assay setup (also evaluated with reference compounds) as described below. Caco-2 cells, at passage number 36, were used in the transport experiments. The cells were purchased from the American Type Culture Collection (Middlesex, UK). Caco-2 cells were seeded in 96-well plates (12,000 cells/well) and cultured for 21 days on cell culture transwell inserts (Transwell). The integrity of the cell monolayer was determined using Lucifer yellow measured in an Envision multilabel reader at Ex/Em 428/535 nm. Transepithelial electrical resistance was also measured to determine the integrity of the cell barrier. The transepithelial electrical resistance value was above 230 ohms $\times$ cm^2 in all experiments.

The permeability of the test compound (at 10 μM) over a Caco-2 cell monolayer from the apical to the basolateral compartment (A to B) was investigated in duplicates over a period of 120 minutes. Hank's Balanced Salt Solution (HBSS), pH 6.5, containing 25 mM of morpholino ethane sulfonic acid (MES) was used as the apical buffer, and HBSS, pH 7.4, containing 25 mM of HEPES and 1% bovine serum albumin (BSA) as the basolateral buffer. The test compound (10 μM) in apical buffer was added to the apical well. Incubation was performed at 37°C, and the plates were kept shaking at approximately 150 rpm. At the 30-minute time point, an aliquot of basolateral sample was collected and replenished with the same volume of basolateral buffer. At 120 minutes, samples were collected from the basolateral and apical chambers. The donor samples were diluted with basolateral buffer (1:1, v/v), and the receiver samples were diluted with apical buffer (1:1, v/v). Possible efflux of test compound was investigated by blocking the MDR1 and BCRP efflux pumps in the A to B assay using 5μM GF120918 (Elacridar) (GF).

In apical to basolateral (ABBA) experiments, the bidirectional permeability of test compound (at 10 μM) through a Caco-2 cell monolayer from the apical to the basolateral compartment and from the basolateral to the apical compartment was investigated in duplicate samples over a period of 120 minutes. HBSS, pH 7.4, containing 25 mM of HEPES was used as a buffer in the ABBA experiments. The test compound (10 μM) in ABBA buffer was added to apical wells (A-B experiment) and to basolateral wells (B-A experiment). Aliquots were collected and treated in the same manner as described above.

All samples were precipitated with four volumes of acetonitrile, containing losartan as the internal standard, and vortexed for 5 minutes at 1000 rpm, followed by centrifugation at 4000 rpm for 10 minutes. Aliquots of the supernatants were analyzed by liquid chromatography tandem mass spectrometry (see below).

The apparent permeability was calculated as follows:

$$P_{app} = \frac{{}^{dQ}/_{dt}}{C_0 \times A} \quad (1)$$

where C_0 is the donor concentration at time 0 and A is the surface area and dQ/dt is the total amount of test compound transported across the cells per unit time.

Estimated +GF/-GF ratios of >1.5 and efflux ratios >2 were considered as an indication of efflux, based on validation using a set of reference P-gp substrates (Giacomini et al., 2010).

Determination of In Vitro Intrinsic Clearance. Determination of the in vitro intrinsic clearance (CL_{int}) in HLM was performed at Medivir or at GVK Biosciences Limited (Hyderabad, India) using identical assay setup (also evaluated with reference compounds) as described below. Pools of HLM from 50 donors (mixed genders) were purchased from XenoTech, LLC (Kansas City, US) and stored at -80°C. The microsomes were diluted in 100 mM of phosphate buffer, pH 7.4. The final concentrations were 1 μM of test compound and 0.5 mg of microsomal protein per mL. Duplicate samples were pre-incubated for 10 minutes at 37°C before starting the reactions by the addition of nicotinamide adenine dinucleotide phosphate to a final concentration of 1 mM (the total incubation volume was 250 μl). The incubations were stopped by the removal of aliquots (25 μl) at 0, 5, 15, 30, and 45 minutes to 96-well plates on ice containing 200 μl of stop solution to precipitate proteins. The stop solution, ice-cold acetonitrile, contained losartan (100 nmol/L) as an analytical internal standard. Samples were left on ice for at least 30 minutes to precipitate the microsomal proteins before removing the precipitate by centrifugation for 20 minutes at 2250 g. Aliquots of the supernatants were analyzed by liquid chromatography tandem mass spectrometry (see below).

The CL_{int} values were obtained from the disappearance curves where the substrate concentration was plotted against the time. The concentration of each test compound in the incubation was fitted to a first-order elimination equation

$$C = C_0 \cdot e^{-k \cdot \Delta t} \quad (2)$$

where C is the measured concentration at time t, C_0 is the concentration at time 0 and k is the elimination constant. Curve fit was performed after natural logarithm transformation of the concentration data.
Intrinsic clearance was calculated as follows:

$$CL_{int} = k \cdot V \quad (3)$$

where V is the volume of the microsomal incubation.
The AP model for metabolic stability in microsomes (CYP_HLM_Clint) is based on the free concentration in the incubation. Since the measured CL_{int} values are based on total concentrations and the fraction unbound in microsomes was not known, the predicted values obtained using the AP model were converted to total as follows:

$$Total\ CL_{int} = Unbound\ CL_{int} \times (S + fu_{mic}) \quad (4)$$

where $S+fu_{mic}$ is the predicted fraction unbound in the microsomal incubation (AP model). The $S+fu_{mic}$ model is largely based on a publication by Austin et al. (2002).

Bioanalysis. The test compounds in the CL_{int} and permeability assays were quantified by LC/MS-MS (Sciex AB, Stockholm, Sweden or Shimadzu, India), in principle as described by Sohlenius-Sternbeck et al. (2010). The compounds were detected in positive or negative electrospray multiple reaction monitoring mode. Optimizations (parent ion and fragment determination, declustering potentials and collision energy) were performed in advance.

Quality Controls. Since the different assays were run in early screening, project compounds were run in one or two separate experiments. Reference compounds were always included in the different experiments as quality controls and to confirm reproducibility over time and between the Medivir and GVK Bio laboratories. Ketoconazole, metoprolol, and propranolol were used as quality controls in every LogD experiment, since the LogD range of these compounds covers the LogD for most Medivir compounds. Albendazole and diethylstilbestrol were used as quality controls for solubility since these compounds cover the low concentration range ($\leq$10 μM) applied in most in vitro ADME assays, and flurbiprofen was chosen as a quality control for high solubility. Atenolol, digoxin, and propranolol were used as permeability quality controls, since these compounds cover the low to high permeability range. Digoxin and quinidine were used as quality controls for efflux in every Caco-2 + GF experiment and in every ABBA experiment. As a quality control in all HLM experiments each experiment included incubations containing a cocktail of probe substrates for human drug-metabolizing enzymes, i.e., phenacetin (for CYP1A2), diclofenac (CYP2C9), bufuralol (CYP2D6), and midazolam (CYP3A4). Criteria for rejecting an experiment was based on whether data were outside two standard deviations of the Manhattan mean. Only project data from accepted experiments were used. For quality control data obtained in the different assays, see Supplemental Table 1, A–E.

Bin Categorization. Bin categorization was performed to evaluate the solubility, metabolic stability, and permeability predictions. For solubility, bin A

contained compounds with poor solubilities (<10 μM) that might precipitate in the in vitro assays and bin D "good" solubilities (>90 μM, close to the added final concentration in the assay), which should suffice for most discovery studies except safety studies. Two other bins were created for practical reasons since some in vitro assays at Medivir were performed at up to 50 μM.

In early discovery, we did not apply strict cut-offs for CL_{int} values, since the compounds are often improved in the optimization phase. An HLM CL_{int} value less than 15 μl/min/mg, was considered stable enough (bin A) to be of interest. A CL_{int} value higher than 50 μl/min/mg can be considered to predict a low bioavailability over the liver, but since there is a fairly large uncertainty in the predictions, we raised the cut-off for bin D to >80 μl/min/mg. Predicted values between 15 and 80 μl/min/mg were arbitrarily divided into 2 bins to differentiate between closer to "stable" (15-30 μl/min/mg, bin B) and closer to "unstable" (30-80 μl/min/mg, bin C).

The measured apparent permeability (P_{app}) values were also divided into 4 categories, A—D (<2, 2–5, 5–10 and $>10 \times 10^{-6}$ cm/s) and the corresponding categories A–D used for P_{eff} predictions were <1, 1–2, 2–3 and >3 (10^{-4} cm/s). The bin borders were set based on historic in-house data for reference compounds.

Statistics. The root–mean–square error (RMSE) was calculated as a measure of the error of a model according to the equation below.

$$RMSE = \sqrt{\frac{\sum_{i=1}^{N}(Predicted - Observed)^2}{N}} \quad (5)$$

where N is the number of compounds in the dataset.

The mean absolute error (MAE) was calculated as a measure of the mean absolute difference between predicted and observed data according to the equation below.

$$MAE = \frac{\sum_{i=1}^{N} abs(Predicted - Observed)}{N} \quad (6)$$

Criteria for Accepting an Experiment. The mean ± SD values for each quality control, obtained from at least 12 independent measurements, were used to define whether an experiment could be accepted. An experiment was rejected if data were outside two standard deviations of the Manhattan mean.

Confusion Tables for Calculation of Precision, Sensitivity, Specificity, and Accuracy. For the 2×2 confusion tables based on P-gp "Yes/No" and Caco-2 P_{app} or ABBA, the precision, sensitivity, specificity, and accuracy were calculated, where TY is predicted True "Yes", TN is predicted True "No", FY is predicted False "Yes", and FN is predicted False "No".

Precision (or predictive value) is the proportion of predicted "Positives" that are true "Positives":

$$Precision = \frac{Predicted\ TY}{(Predicted\ TY\ +\ Predicted\ FY)} \quad (7)$$

Sensitivity (or recall) is the proportion of actual "Positives" that were correctly predicted:

$$Sensivity = \frac{Predicted\ TY}{(Predicted\ TY\ +\ Predicted\ FN)} \quad (8)$$

Specificity is the proportion of actual "Negatives" that were correctly predicted:

$$Specificity = \frac{Predicted\ TN}{(Predicted\ TN\ +\ Predicted\ FY)} \quad (9)$$

Accuracy is the proportion of data that was correctly predicted:

$$Accuracy = \frac{(Predicted\ TY\ +\ Predicted\ TN)}{(Predicted\ TY\ +\ Predicted\ TN\ +\ Predicted\ FY\ +\ Predicted\ FN)} \quad (10)$$

For the 4×4 confusion tables for the three models built with four categories (solubility, metabolic stability and permeability), precision (predictive value) and sensitivity (recall) were calculated for each bin. The F1-score for each bin is the harmonic mean of precision and recall, i.e.,

$$F1 - score = \frac{2 \times precision \times recall}{(precision\ +\ recall)} \quad (11)$$

The bin sizes, for the total data set as well as for the test set for each model, are shown in Table 1. Since we had unbalanced categories, we also used the Weighted F1 for overall "accuracy", which takes the weighted mean of the individual F1-scores, considering the number of values in each measured category, i.e., the sum of the F1-scores for each measured category times the number of compounds in that category divided by the total number of compounds in the dataset.

$$\begin{aligned} Weighted\ F1\ =\ &((F1_A \times\ measured\ cpds_A) \\ &+\ (F1_B\ \times\ measured\ cpds_B) \\ &+\ (F1_C\ \times\ measured\ cpds_C) \\ &+\ (F1_D\ \times\ measured\ cpds_D))/(measured\ cpds_A \\ &+\ measured\ cpds_B\ +\ measured\ cpds_C \\ &+\ measured\ cpds_D) \end{aligned} \quad (12)$$

Results

LogD Predictions. The total number of compounds with measured LogD was 1198. Fig. 2A shows the S+LogD, predicted by the global model provided in AP, versus the observed LogD for all compounds. The R^2 value was 0.79 (See also Table 2). A local, in-house model, based on a training set (911 compounds) from the Medivir data were built using the AP Modeler module, and Fig. 2B shows the predicted LogD versus the observed LogD when this local model was used for the 287 compounds in the test set. The same test set was

TABLE 1

Bin size for the datasets. The measured solubilities were divided into 4 categories, (A–D) (<10, 10–50, 50–90 and >90 μM) and the same categories were used for binning the predictions. The measured CLint values were divided into four categories, (A–D) (<15, 15–30, 30–80 and >80 μl/min/mg) and the same categories were used for binning the predictions. The measured apparent permeability values were divided into 4 categories, (A–D) (<2, 2–5, 5–10 and $>10 \times 10^{-6}$ cm/s) and the corresponding categories (A–D) used for effective jejunal permeability predictions were <1, 1–2, 2–3 and >3 (10^{-4} cm/s).

Parameter Predicted	Model	Data Set	Tot cpds	Tot Correctly Predicted	Predicted Bin Size				Measured Bin Size			
					Bin A	Bin B	Bin C	Bin D	Bin A	Bin B	Bin C	Bin D
Solubility	AP	All	2778	1553	69	241	201	2267	582	319	340	1537
	AP	Test	691	410	13	46	47	585	101	78	92	420
	local	Test	691	221	92	140	404	55	101	78	92	420
Metabolic stability	AP	All	4794	1779	973	1586	1444	791	1332	598	941	1923
HLM CL_{int}	AP	Test	1199	442	231	385	382	201	340	135	232	492
	local	Test	1199	766	235	236	309	419	340	135	232	492
Permeability	AP, P_{eff}	All	2586	1114	1072	856	341	317	962	306	399	919
Caco-2 P_{app}	AP, P_{eff}	Test	516	245	220	154	72	70	204	61	78	173
	local, P_{app}	Test	516	317	166	90	87	173	204	61	78	173

AP, ADMET Predictor; CL_{int}, in vitro intrinsic clearance; P_{eff}, effective jejunal permeability; P_{app}, apparent permeability; Tot cpds, total number of compounds.

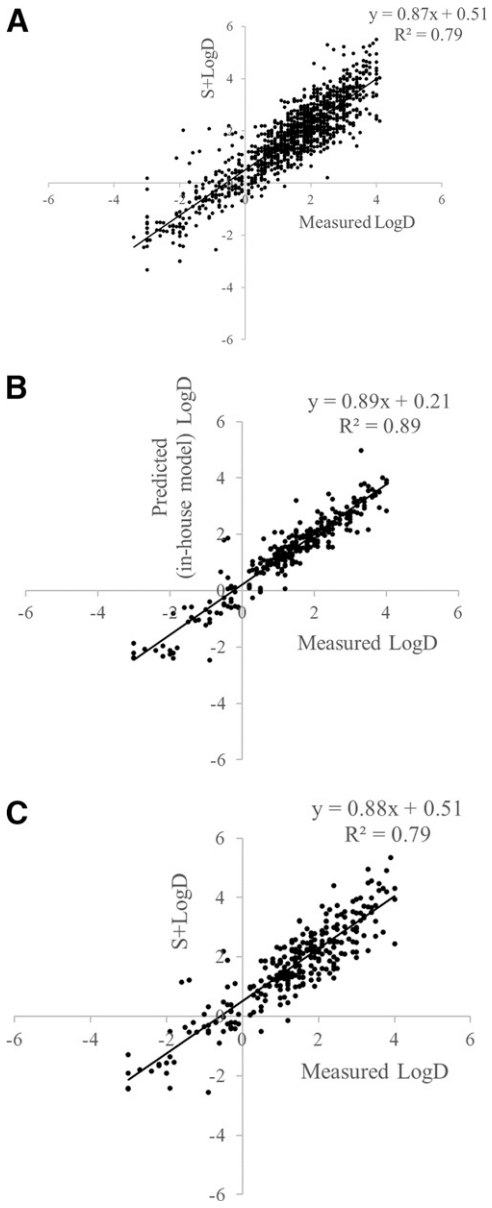

Fig. 2. Predicted LogD versus measured LogD using (A) the global S+LogD model (ADMET Predictor model) for all 1198 compounds with measured values, (B) the in-house (local) model for the test set (287 compounds), and (C) the S+LogD model for the test set.

also predicted with the global AP model, S+LogD (Fig. 2C). The R^2 values, when performing linear regression for the predicted values versus the measured values for the test set, using the S+LogD and the in-house LogD model, were 0.79 and 0.89, respectively (Table 2).

Solubility Predictions. The total number of compounds with measured solubility was 2778. The measured solubilities were divided into 4 categories, A-D (<10, 10–50, 50–90 and >90 μM) and the same categories were used for binning the predictions and a 4×4 confusion table constructed. 55% of all measured values were in the highest category, i.e., >90 μM, and 21% in the lowest category, i.e., <10 μM (Table 1). When using the global AP model for all 2778 compounds, <3% (i.e., 69 compounds) had a predicted solubility of <10 μM (Table 1). Almost 82% of all compounds were predicted to have a solubility >90 μM. However, 56% of all compounds were correctly predicted, when taking all categories into consideration, and many were close to the border between the categories (Table 3).

TABLE 2

Prediction outcome for the ADMET Predictor models and the in-house models for compounds in the Medivir dataset.

Assay	Total Number of Compounds	Number of Compounds in Training Set	Number of Compounds in Test Set	AP Model (All Compounds)			AP Model (Test Tet)			In-House Model (Test Set)		
				RMSE	MAE	R^2	RMSE	MAE	R^2	RMSE	MAE	R^2
LogD	1198	911	287	0.771	0.589	0.785	0.757	0.585	0.790	0.488	0.349	0.888
Solubility*	2778	2087	691	1.261	1.075	0.260	1.229	1.055	0.202	0.388	0.247	0.593
HLM CL_{int}*	4794	3595	1199	0.566	0.454	0.531	0.574	0.462	0.498	0.327	0.250	0.717
Caco-2 permeability*	2586	2070	516	NA	NA	NA	NA	NA	NA	0.370	0.265	0.614

*Model based on logarithmic data.
AP, ADMET Predictor; HLM, human liver microsomes; MAE, mean absolute error; RMSE, root mean square error.

TABLE 3

Precision, sensitivity, and F1-score for each bin as well as overall accuracy and weighted F1 for the global models with the total datasets and for the in-house and global models with the test sets. The measured solubilities were divided into four categories, A–D (<10, 10–50, 50–90 and >90 μM), and the same categories were used for binning the predictions. The measured CL_{int} values were divided into four categories, A–D (<15, 15–30, 30–80 and >80 μl/min/mg), and the same categories were used for binning the predictions. The measured apparent permeability values were divided into four categories, A—D (≤2, 2–5, 5–10 and >10 × 10^{-6} cm/s) and the corresponding categories A–D used for effective jejunal permeability predictions were <1, 1–2, 2–3 and >3 (10^{-4} cm/s).

Parameter Predicted	Model	Data Set	Tot cpds	Accuracy (Tot Correct) in %	Precision (Predictive Value) or Predicted Bin, Correct Prediction				Sensitivity or Recall Measured Bin, Correctly Predicted				F1-Score				Weighted F1
					Bin A	Bin B	Bin C	Bin D	Bin A	Bin B	Bin C	Bin D	Bin A	Bin B	Bin C	Bin D	
Solubility	AP	All	2778	56	0.68	0.14	0.11	0.64	0.08	0.10	0.06	0.94	0.14	0.12	0.08	0.76	0.48
	AP	test	691	59	0.54	0.09	0.15	0.67	0.07	0.05	0.08	0.93	0.12	0.06	0.10	0.78	0.51
	local	test	691	32	0.77	0.29	0.15	0.91	0.70	0.51	0.65	0.12	0.74	0.37	0.24	0.21	0.31
Metabolic Stability	AP	All	4794	37	0.55	0.16	0.26	0.79	0.40	0.42	0.40	0.32	0.46	0.23	0.31	0.46	0.40
	AP	test	1199	37	0.54	0.16	0.26	0.78	0.36	0.47	0.42	0.32	0.43	0.24	0.32	0.45	0.40
HLM CL_{int}	local	test	1199	64	0.85	0.28	0.43	0.87	0.59	0.50	0.58	0.74	0.70	0.36	0.50	0.80	0.66
Permeability	AP, P_{eff}	All	2586	43	0.64	0.16	0.18	0.72	0.72	0.44	0.16	0.25	0.68	0.23	0.17	0.37	0.44
Caco-2 P_{app}	AP, P_{eff}	test	516	47	0.68	0.19	0.24	0.69	0.74	0.49	0.22	0.28	0.71	0.28	0.23	0.40	0.48
	local, P_{app}	test	516	61	0.89	0.30	0.25	0.69	0.73	0.44	0.28	0.69	0.80	0.36	0.27	0.69	0.63

AP, ADMET Predictor; CL_{int}, in vitro intrinsic clearance; HLM, human liver microsomes; P_{app}, apparent permeability; P_{eff}, effective jejunal permeability; Tot cpds, total number of compounds.

Fig. 3. Predicted solubility versus measured solubility in four categories using (A) the global S+S_pH model at pH 7.4 (ADMET Predictor model) for all 2778 compounds with measured values, (B) the in-house (local) model for the test set (691 compounds), and (C) the global S+S_pH model for the test set. For each bin, the number of compounds with predicted solubility in the specified range is presented as percentage of total compounds in the bin. Note that for the S+S_pH model, the solubility was converted from mg/ml to μM.

A training set consisting of 2087 of the compounds was used to build an in-house local solubility model using the AP Modeler module. The remaining 691 compounds were the test set. Seventy-one of the 101 compounds (70%) that had a measured solubility <10 μM were also predicted to be poorly soluble (<10 μM, See Fig. 3B and Table 3). Only 12% of the highly soluble (>90 μM) compounds were predicted to have solubility >90 μM, but 73% were predicted to have a fairly high solubility (50-90 μM, See Fig. 3B).

Table 2 summarizes the statistics for the linear regression for the plot of predicted versus measured solubility based on logarithmic data for these compounds. The R^2 value was 0.59 for the in-house model and lower for the AP model (i.e., 0.20 for the test set and 0.26 when using all compounds). The Precision (Predictive value), Sensitivity (Recall), and F1-score (per bin) for the categories and the overall accuracy (and Weighted F1) for all models are presented in Table 3. With the global model, the precision (or predictivity) was similar for bin A (low solubility, <10 μM) and bin D (high solubilities, >90 μM) with values between 0.54 and 0.68 when using all compounds or just the test set, indicating that the test set was representative. Also, both precision and sensitivity were similar for bins B and C using the global model, and the F1 score was around 0.8 for bin D and below >0.15 for Bins A–C. With the in-house model, the precision for low-solubility compounds was 0.77 and for high-solubility it was 0.91. The sensitivity was 0.70 for low solubility compounds but only 0.12 for high-solubility compounds with the in-house model. Also, the F-score was high (0.74) for low-solubility compounds and low for high-solubility compounds (0.21). A total of 32% were correctly predicted with the category boundaries chosen. When using the global model for the same test set, only 7% of the poorly soluble compounds but 93% of the highly soluble compounds were correctly predicted. Thus, 59% of all test compounds were correctly predicted (Table 3).

Predictions of Metabolic Stability in Human Liver Microsomes. The AP global CYP_HLM_Clint model is based on the unbound concentrations, and these values were therefore converted to total CL_{int} (see Materials and Methods) to compare with the measured values for total CL_{int}. The total number of compounds with measured HLM CL_{int} was 4794. The measured CL_{int} values were divided into 4 categories, A-D (<15, 15-30, 30-80, and >80 μl/min/mg) and the same categories were used for binning the predictions. A 4×4 confusion table was constructed. Around 40% (i.e., 1923 compounds) of the total number of compounds had a measured CL_{int} value >80 μl/min/mg (bin D) and 28% (i.e., 1332 compounds) had a low CL_{int} value, category A (Table 1). Of the 1332 compounds measured to be stable (CL_{int} <15 μl/min/mg), 40% were correctly predicted (Fig. 4A). Of the 973 compounds (20% of all compounds) with a predicted CL_{int} <15 μl/min/mg, 55% were also stable when measured, while around 18% of the compounds were measured to be unstable (i.e., CL_{int} >80 μl/min/mg) in the assay. Overall, 37% of all compounds were correctly predicted (Table 3).

A training set consisting of 3595 of the compounds was used to build an in-house, local metabolic stability model, which was evaluated using the remaining 1199 compounds (i.e., the test set). Of the 340 compounds with measured high stability, 59% were correctly predicted (Fig. 4B). 87% of the compounds with a predicted CL_{int} >80 μl/min/mg had a measured value in the same range. Of the compounds with a predicted low CL_{int} (i.e., <15 μl/min/mg), 85% had a measured low CL_{int}, and less than 0.5% had a measured CL_{int} >80 μl/min/mg. Overall, 64% of the compounds in the test set were correctly predicted. When using the global AP model for predictions with the same test set, 37% of the compounds were correctly predicted (Table 3 and Fig. 4C). The prediction success is summarized in Table 2, demonstrating that the in-house model had a higher R^2 value (i.e., 0.71) than the global model (i.e., around 0.5 regardless if using all compounds or the test set).

The CYP_HLM_Clint model and the in-house CL_{int} model were also used to predict CL_{int} for a set of commercially available compounds with in-house measured data (the results are listed in Supplemental Table 2). The prediction success is shown in Table 4, demonstrating that the in-house model had a higher R^2 value (i.e., 0.51) than the global model (i.e., 140).

Permeability. The total number of compounds with measured Caco-2 P_{app} was 2586. Since the main AP software does not have a Caco-2 model, permeabilities were predicted with the global AP $S+P_{eff}$ model and compared with the measured Caco-2 values. The Membrane Plus or GastroPlus software, both from Simulations Plus, could be used to predict P_{app} values. We did not have access to

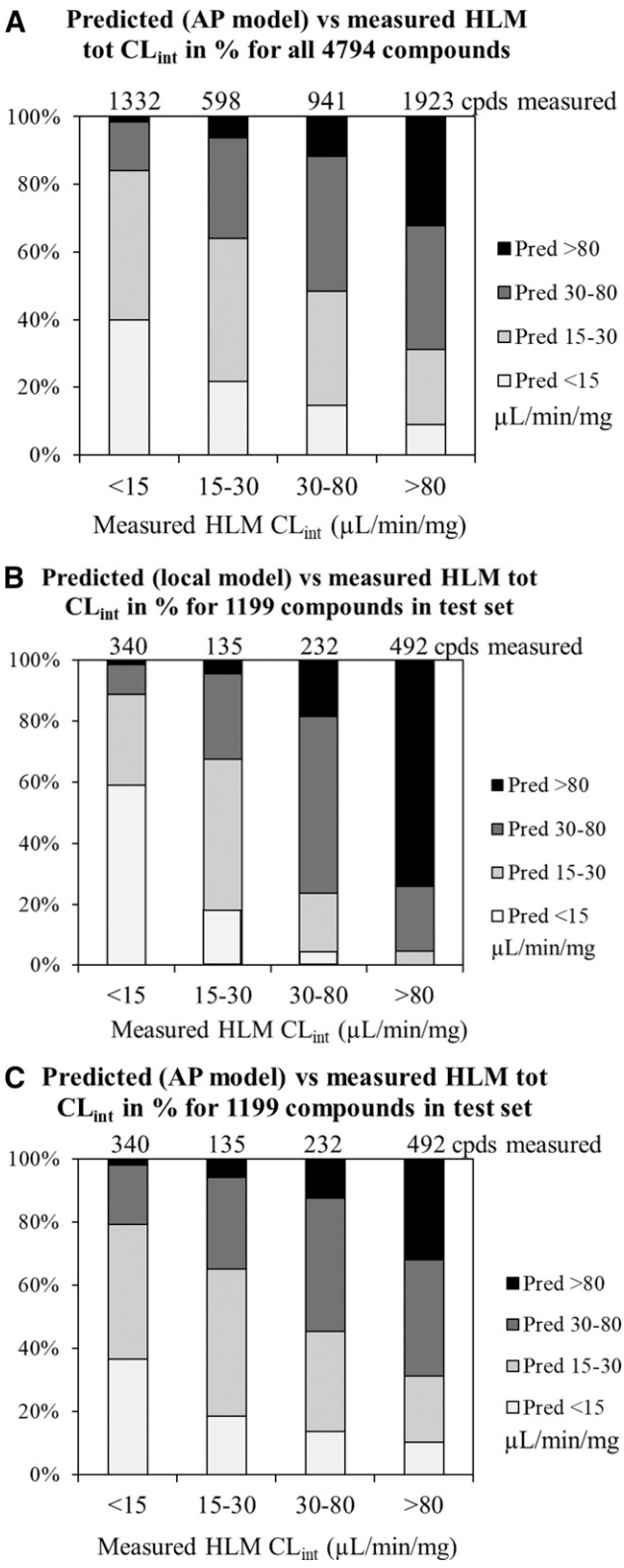

Fig. 4. Predicted in vitro intrinsic clearance (CL_{int}) versus measured CL_{int} in four categories using (A) the global CYP_HLM_Clint model (ADMET Predictor model), versus measured total HLM CL_{int} for all 4794 compounds with measured values, (B) the in-house (local) model for the test set (1199 compounds), and (C) the global CYP_HLM_Clint model for the test set. For each bin, the number of compounds with predicted CL_{int} in the specified range is presented as percentage of total compounds in the bin. Note that the predicted CL_{int} from the CYP_HLM_Clint was converted to total CL_{int}) using the predicted $S+fu_{mic}$ (global ADMET Predictor model).

TABLE 4

Prediction outcome for CL_{int} in HLM and Caco-2 with the AP models and the in-house models for commercially available reference compounds with in-house measured data (See Supplemental Tables 2 and 3).

		AP Model			In-House Model		
Assay	Number of Compounds	RMSE	MAE	R^2	RMSE	MAE	R^2
Human liver microsomal CL_{int}	75	0.454	0.333	0.140	0.313	0.247	0.512
Caco-2 permeability	26	NA	NA	NA	0.333	0.265	0.782

Analysis based on logarithmic data.
NA: Not available since the ADMET Predictor (AP) model predicted effective jejunal permeability (P_{eff}), not apparent permeability (P_{app}).

these in this study. The local Caco-2 P_{app} model was built in the AP Modeler module using inhouse P_{app} data only.

When using all the compounds, 72% of the compounds with a measured P_{app} value of $\leq 2 \times 10^{-6}$ cm/s had a predicted P_{eff} value of $< 1 \times 10^4$ cm/s as shown in Fig. 5A and Table 3. Of the compounds with a predicted human effective permeability in the jejunum, S+P_{eff}, of $< 1 \times 10^4$ cm/s, 64% demonstrated a measured apparent permeability in Caco-2, P_{app}, of $\leq 2 \times 10^{-6}$ cm/s (Table 3). Forty-three percent of the compounds were correctly predicted using the AP P_{eff} model and these categories.

A training set consisting of 2070 compounds was used to build an in-house, Caco-2 P_{app} model, which was evaluated using the remaining 516 compounds. Table 2 summarizes the statistics for the linear regression for the plot of predicted versus measured Caco-2 P_{app} based on logarithmic data. The R^2 value was 0.61 for the in-house model (a R^2 value for the global model could not be obtained since the global model provides a P_{eff} value). Eighty-nine percent of the compounds in the test set with a predicted $P_{app} \leq 2 \times 10^{-6}$ cm/s had a measured value in the same range (Table 3). Of the compounds with a predicted high P_{app} (i.e., $> 10 \times 10^{-6}$ cm/s), 69% also had a measured high P_{app}. The in-house model predicted 61% of the test set correctly. When the global P_{eff} model was used to predict Caco-2 P_{app} categories for the test set, 47% were correctly predicted based on the bin categorization. The sensitivity with both models was around 0.7 for low-permeability compounds but lower for high-permeability compounds.

The in-house model was also used to predict P_{app} for a set of commercially available reference compounds with in-house measured data (Supplemental Table 3). Table 4 shows that the R^2 for the regression (based on logarithmic data) was 0.78 (See Supplemental Table 4 for analysis of variance).

The prediction of P-gp substrates was also investigated. Predicted P-gp substrate ("yes") was compared with a +/− P-gp inhibitor ratio of >1.5 in the Caco-2 assay, and with an ABBA ratio of >2.0 (Table 5). The precision, sensitivity, specificity, and accuracy of these predictions were 75%, 96%, 30%, and 75%, respectively, when compared with the P-gp inhibitor ratio, and 93%, 93%, 22%, and 86%, respectively, when compared with the ABBA ratio.

Discussion

In the present study, the evaluations of the global AP models for LogD, water solubility, metabolic stability in HLM, and intestinal permeability were performed with experimental data from a total of 4794 Medivir compounds (not all compounds had measured data for all parameters). Also, in-house local models were built by using artificial neural network (ANN) models in the optional Modeler module of AP. For each parameter, approximately 75–80% of the Medivir data were used as a training set, and the remaining compounds were used as a test set. With the global model, the test set and total dataset for each parameter gave similar precision and sensitivity, indicating that the test sets were representative.

Of the AP global models tested in this study, the S+LogD model demonstrated the best agreement with observed data (Table 2). This is likely explained by good agreement in assay output across laboratories, since the assay setup for the octanol-water partition assay is straightforward and not dependent on any biologic test systems. The prediction success was somewhat better with the in-house local LogD model compared with the global model (Table 2).

Solubility is an important parameter for the bioavailability of drugs. Different methods are used for measuring solubility, e.g., thermodynamic solubility, kinetic solubility, and dried DMSO solubility (Alelyunas et al., 2009; Saal and Petereit, 2012). Predictions of solubility are challenging since it is difficult to obtain consistent data for model building. In this work, we used a set of in-house data obtained with a kinetic solubility assay performed at pH 7.4, based on 10 mM of compounds in DMSO stock solutions, relevant for most early screening assays in which compounds with solubility values below 10 μM may precipitate. Unless high therapeutic concentrations will be needed, solubilities >90 μM should be sufficient for preclinical assays and studies (even though high doses in safety studies in vivo may still be challenging). However, this solubility will not be relevant for other formulations in later phases. Our data set was unbalanced, with a majority of compounds having high solubility. Only a small proportion (<3%) predicted solubility below 10 μM using the global model, even though the dataset contained 21% compounds with low solubility. Moreover, most compounds with a low measured solubility had a high predicted solubility value using the global AP model. Thus, the S+S_pH (at pH 7.4) model was not very useful for filtering out the poorly soluble compounds for in vitro drug metabolism and pharmacokinetics (DMPK) for the Medivir dataset. However, approximately 56% of the compounds were still predicted correctly due to the large proportion of compounds with high solubility.

The prediction success for low solubility compounds was improved when the in-house local model was used. The global model overpredicted solubility, and the in-house local model was better at identifying the low-solubility compounds which could cause assay problems but underpredicted highly soluble compounds (see F1-scores, Table 3). However, with a majority of compounds having high solubility, the total number of correctly predicted compounds was lower for the in-house model than for the global model (Fig. 3B and weighted F1 in Table 3).

Later in drug development, more accurate solubility measurements in relevant formulations and biologic matrices will be important. In AP, the solubility can be predicted at different pHs and also in some biologically relevant matrices, such as fasted state simulated gastric fluid, fasted state simulated intestinal fluid, and fed state simulated gastric fluid which, if low, can help to explain one major reason for poor oral bioavailability in vivo.

Early screening of metabolic stability in HLM is routinely performed in drug discovery, since the metabolism of a compound will affect its overall pharmacokinetics (Sohlenius-Sternbeck et al., 2016). The prediction success for high- and low-CL_{int} compounds was increased when the in-house local model was used. However, none of the prediction models predicted CL_{int} accurately in the range between low and high metabolic stability and do not give a reliable CL_{int} value for scaling to in vivo, but the models can be useful for categorization of high and low metabolic stability. Predicted values in the range of 15–30 μl/min/mg often had measured values <15 μl/min/mg (Figs. 4A and B). This information could still be useful for most early projects, when trying to design metabolically stable compounds.

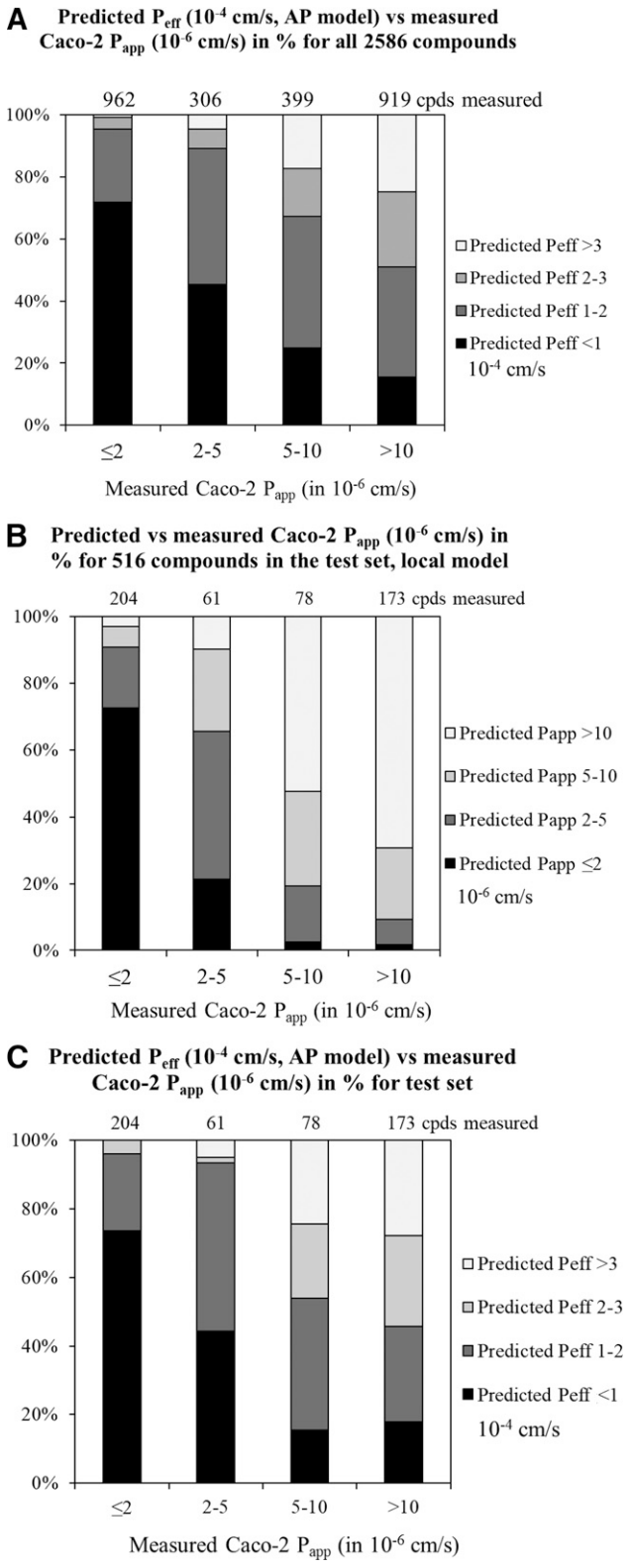

Fig. 5. Predicted intestinal permeability (effective jejunal permeability, P_{eff}, or apparent permeability, P_{app}) versus measured Caco-2 P_{app} in 4 categorizes using (A) the S+P_{eff} model (ADMET Predictor model) for all 2586 compounds with measured P_{app} values, (B) the in-house (local) model for the test set (516 compounds), and (C) the S+P_{eff} model for the test set. For each bin, the number of compounds with predicted P_{eff} or P_{app} in the specified range is presented as percentage of total compounds in the bin.

The AP and in-house models for metabolic stability were also tested with a set of reference compounds. These are commercially available compounds and may have been part of the training dataset for the AP global model. Nevertheless, the prediction outcome demonstrated higher R^2 for the in-house model compared with the AP model (Table 4), although the structures for the in-house training set were dissimilar to the reference compounds. This may be due to experimental assay conditions being the same for the reference compounds and the in-house compounds in the training set, while the data for the training set in the AP global model may have come from several different experimental setups.

Intestinal permeability measurements are important for the understanding of absorption and bioavailability of oral drugs. The Caco-2 cell line is commonly used to measure apparent intestinal permeability and to give an indication of human absorption (Artursson et al., 2001). However, the permeability in Caco-2 cells is highly dependent on the experimental conditions (Hayeshi, 2008). There was no Caco-2 model available in the main AP software. However, Simulations Plus has prediction models in GastroPlus and MembranePlus. In this work, we used the global AP P_{eff} model to predict measured Caco-2 P_{app} values. Predicted P_{eff} values of 1 and 3.0×10^{-4} cm/s could be used as cut-offs for low and high permeability, respectively. However, it is difficult to use predicted values between 1 and 3.0×10^{-4} cm/s to convert to specific Caco-2 P_{app} values or to predict the absolute absorption in vivo for moderate values. In early discovery, the model could still be used to indicate very low and high permeability compounds. The in-house P_{app} model showed improved predictions for the test set, compared with the AP P_{eff} model, for low permeabilities (Table 3). The global model showed somewhat lower precision for low-permeability compounds. Both the global P_{eff} model and the in-house P_{app} model could be useful tools to identify structures with likely low permeability, for the Medivir compounds, and to guide design and synthesis of more permeable compounds.

The in-house model for permeability was also tested with a set of commercial reference compounds, demonstrating similar prediction outcome as for the Medivir dataset with an R^2 value of 0.73 (Table 4).

The AP model for P-gp substrate identification was evaluated based on measured values of effect of P-gp inhibition and efflux ratio in ABBA. The P-gp model identified a large proportion of the compounds that were also shown to be P-gp substrates in the in vitro assays, giving high sensitivity and accuracy in confusion tables (see Table 5). However, chemical series with compounds that were P-gp substrates were overrepresented in the study (68%), and the reason for the low specificity number can be explained by the low number of negative data in the dataset.

Our evaluation shows that the global AP models can be used for rough categorization of high and low values in early discovery, based on predicted results for metabolic stability in HLM and P_{eff} permeability, and to give accurate predictions of Log D, guiding the synthesis of new compounds and for prioritizing in vitro ADME experiments. The model seems to overpredict solubility for Medivir compounds, however. It can be useful to also look at pH- and matrix-dependent solubility models in AP. Local in-house prediction models built with the optional AP Modeler Module can improve predictions. As more data are generated, the in-house models will likely have to be rebuilt, when structures move away from the initial training set.

Predictions of advantageous ADME properties should trigger further experimental evaluations. There is often a trade off with efficacy and toxicity so, if in vitro efficacy is promising, selected compounds with poor predicted properties should be experimentally tested in ADMET

TABLE 5

Confusion tables demonstrating AP performance in predicting P-gp substrates for the 387 Medivir compounds tested in the P-gp inhibitor assay and in predicting P-gp substrates for the 103 Medivir compounds tested in the ABBA assay. Predicted P-gp substrate ("yes") was compared with a measured + P-gp inhibitor/- P-gp inhibitor ratio of >1.5 and with an ABBA ratio of >2.0. The total number of compounds with a measured ratio >1.5 in the +P-gp inhibitor/-P-gp inhibitor assay was 264 (i.e., 68% of compounds tested), and the total number of compounds with a measured ratio >2 in the ABBA assay was 94 (i.e., 91% of compounds tested).

Caco-2 Assay Setup	TY	FY	TN	FN	Precision TY/(TY+FY)	Sensitivity TY/(TY+FN)	Specificity TN/(TN+FY)	Accuracy (TY+TN)/Total
+/− P-gp inhibitor	254	86	37	10	0.75	0.96	0.30	0.75
ABBA	87	7	2	7	0.93	0.93	0.22	0.86

ABBA, apical to basolateral and basolateral to apical; FN, predicted False "No"; FY, predicted False "Yes"; TN is predicted True "No"; TY, predicted True "Yes."

assays to confirm the predictions and be balanced against potency, toxicity, predicted dose and dosing regimen. Depending on the specific project criteria, such as indication, dose, and intended dosing regimen, a project can, of course, accept compounds with some poor properties.

Acknowledgment

The authors thank Dr. Fredrik Öberg, Chief Scientific Officer at Medivir AB, for allowing us to use these data.

Authorship Contributions

Participated in research design: Sohlenius-Sternbeck, Terelius.

Performed data analysis: Sohlenius-Sternbeck, Terelius.

Wrote or contributed to the writing of the manuscript: Sohlenius-Sternbeck, Terelius.

References

Alelyunas YW, Liu R, Pelosi-Kilby L, and Shen C (2009) Application of a Dried-DMSO rapid throughput 24-h equilibrium solubility in advancing discovery candidates. *Eur J Pharm Sci* **37**:172–182.

Alqahtani S (2017) In silico ADME-Tox modeling: progress and prospects. *Expert Opin Drug Metab Toxicol* **13**:1147–1158.

Artursson P, Palm K, and Luthman K (2001) Caco-2 monolayers in experimental and theoretical predictions of drug transport. *Adv Drug Deliv Rev* **46**:27–43.

Austin RP, Barton P, Cockroft SL, Wenlock MC, and Riley RJ (2002) The influence of nonspecific microsomal binding on apparent intrinsic clearance, and its prediction from physicochemical properties. *Drug Metab Dispos* **30**:1497–1503.

Ballard P, Brassil P, Bui KH, Dolgos H, Petersson C, Tunek A, and Webborn PJH (2012) The right compound in the right assay at the right time: an integrated discovery DMPK strategy. *Drug Metab Rev* **44**:224–252.

Giacomini KM, Huang SM, Tweedie DJ, Benet LZ, Brouwer KL, Chu X, Dahlin A, Evers R, Fischer V, Hillgren KM, et al.; International Transporter Consortium (2010) Membrane transporters in drug development. *Nat Rev Drug Discov* **9**:215–236.

Gleeson MP and Montanari D (2012) Strategies for the generation, validation and application of in silico ADMET models in lead generation and optimization. *Expert Opin Drug Metab Toxicol* **8**:1435–1446.

Hayeshi R, Hilgendorf C, Artursson P, Augustijns P, Brodin B, Dehertogh P, Fisher K, Fossati L, Hovenkamp E, Korjamo T, et al. (2008) Comparison of drug transporter gene expression and functionality in Caco-2 cells from 10 different laboratories. *Eur J Pharm Sci* **35**:383–396.

Kazmi SR, Jun R, Yu M-S, Jung C, and Na D (2019) In silico approaches and tools for the prediction of drug metabolism and fate: A review. *Comput Biol Med* **106**:54–64.

Kramer JA, Sagartz JE, and Morris DL (2007) The application of discovery toxicology and pathology towards the design of safer pharmaceutical lead candidates. *Nat Rev Drug Discov* **6**:636–649.

Liu R, Schyman P, and Wallqvist A (2015) Critically Assessing the Predictive Power of QSAR Models for Human Liver Microsomal Stability. *J Chem Inf Model* **55**:1566–1575.

Moda TL, Torres LG, Carrara AE, and Andricopulo AD (2008) PK/DB: database for pharmacokinetic properties and predictive in silico ADME models. *Bioinformatics* **24**:2270–2271.

Saal C and Petereit AC (2012) Optimizing solubility: kinetic versus thermodynamic solubility temptations and risks. *Eur J Pharm Sci* **47**:589–595.

Sohlenius-Sternbeck AK, Afzelius L, Prusis P, Neelissen J, Hoogstraate J, Johansson J, Floby E, Bengtsson A, Gissberg O, Sternbeck J, et al. (2010) Evaluation of the human prediction of clearance from hepatocyte and microsome intrinsic clearance for 52 drug compounds. *Xenobiotica* **40**:637–649.

Sohlenius-Sternbeck AK, Janson J, Bylund J, Baranczewski P, Breitholtz-Emanuelsson A, Hu Y, Tsoi C, Lindgren A, Gissberg O, Bueters T, et al. (2016) Optimizing DMPK Properties: Experiences from a Big Pharma DMPK Department. *Curr Drug Metab* **17**:253–270.

Sohlenius-Sternbeck AK, Meyerson G, Hagbjörk AL, Juric S, and Terelius Y (2018) A strategy for early-risk predictions of clinical drug-drug interactions involving the GastroPlus™ DDI module for time-dependent CYP inhibitors. *Xenobiotica* **48**:348–356.

Stålring J, Sohlenius-Sternbeck AK, Terelius Y, and Parkes K (2018) Confident application of a global human liver microsomal activity QSAR. *Future Med Chem* **10**:1575–1588.

Wang Y, Xing J, Xu Y, Zhou N, Peng J, Xiong Z, Liu X, Luo X, Luo C, Chen K, et al. (2015) In silico ADME/T modelling for rational drug design. *Q Rev Biophys* **48**:488–515.

van de Waterbeemd H and Gifford E (2003) ADMET in silico modelling: towards prediction paradise? *Nat Rev Drug Discov* **2**:192–204.

Yan A and Gasteiger J (2003) Prediction of Aqueous Solubility of Organic Compounds by Topological Descriptors. *QSAR Comb Sci* **22**:821–829.

Address correspondence to: Anna-Karin Sohlenius-Sternebeck, Research Institutes of Sweden, RISE, Forskargatan 20D, SE-151 36 Södertälje, Sweden. E-mail: anna-karin.sternbeck@ri.se

DATA SUPPLEMENTS

Evaluation of ADMET Predictor™ in early discovery DMPK project work

Anna-Karin Sohlenius-Sternbeck and Ylva Terelius

Drug Metabolism and Disposition
DMD-AR-2021-000552

Supplemental Table 1

The first data column in Supplemental Tables 1A-E summarizes quality control data for LogD, kinetic solubility, metabolic stability in HLM and permeability in Caco-2 cells. Criteria for rejecting an experiment is based on whether data is outside two standard deviations of the Manhattan mean. Only data from accepted experiments were used.

1A. Quality control reference data for LogD. The first data column shows the Manhattan mean ± standard deviation from 12 separate experiments.

Quality control reference compound	LogD	Acceptable LogD range in assay	Predicted LogD S+LogD model	In-house LogD model
Ketoconazole	3.21 ± 0.12	3.0-3.45	3.71	3.02
Metoprolol	-0.36 ± 0.07	-0.5-(-0.2)	-0.128	0.03
Propranolol	1.04 ± 0.07	0.9-1.2	0.949	1.09

1B. Quality control reference data for kinetic solubility. The first data column shows the Manhattan mean (± standard deviation for diethylstilbestrol) from 191 separate experiments.

Quality control reference compound	Solubility (µM)	Acceptable kinetic solubility range in assay	Predicted S+S_pH (µM)	In-house solubility model (µM)
Albendazole	<2	<2	60	3.1
Diethylstilbestrol	7.7 ± 1.6	4.5-11	89	53
Flurbiprofen	>95	>95	29074	73

1C. Quality control reference data for metabolic stability in human liver microsomes. The first data column shows the Manhattan mean ± standard deviation from 26 in-house experiments. For predicted values see Supplemental Table 2.

Quality control reference compound	CL_{int} (µl/min/mg)	Acceptable CL_{int} range in assay (µl/min/mg)
Bufuralol	20.6 ± 2.4	16-25
Diclofenac	131 ±12.7	105-156
Midazolam	>300	>300
Phenacetin	10.0 ± 2.3	5-15

CL_{int}, in vitro intrinsic clearance

1D. Quality control reference data for permeability in Caco-2 cells. The first data column shows the Manhattan mean ± standard deviation from 62 separate experiments. For predicted values see Supplemental Table 3.

Quality control reference compound	**P_{app} (10^{-6} cm/s)**	**Acceptable P_{app} range in assay (10^{-6} cm/s)**
Atenolol	<1	<1
Digoxin	1.0 ± 0.6	<2
Digoxin + 5 µM GF*	6.0 ± 1.9	NA
Propranolol	17.9 ± 3.8	10-25

* In the presence of 5 µM GF, a P-gp inhibitor, a 6-fold higher P_{app} was obtained.
NA = Not applicable
GF, GF120918 (Elacridar); P_{app}, apparent permeability

1E. Quality control reference data for permeability in the Caco-2 ABBA assay. The first data column shows the Manhattan mean ± standard deviation from 15 separate experiments.

Quality control reference compound	**ABBA ratio**	**Acceptable ABBA ratio range**	**Predicted P-gp substrate AP model**
Digoxin	15.9 ± 3.8	>2	Yes
Quinidine	3.2 ± 0.9	>2	Yes

ABBA, apical to basolateral and basolateral to apical

Supplemental Table 2.

Measured total CL_{int} in HLM for a set of reference compounds and the predicted CL_{int} using the global AP model for unbound CL_{int} (CYP_HLM_Clint), converted to predicted total CL_{int} using the predicted unbound fraction, S+fu from AP. The last column shows the CL_{int} predictions using the in-house CL_{int} model (built on measured total CL_{int} data). Data is the mean of at least three independent experiments.

Compound	**Measured total CL_{int} (µL/min/mg)**	**CYP_HLM_Clint converted to total CL_{int}(µL/min/mg)**	**In-house HLM total CL_{int} model (µL/min/mg)**
Abexinostat	6.0	10.2	10.0
Acetaminophen	6.0	21.6	7.3
Aliskiren	20.0	13.1	54.4
Amitriptyline	83.0	18.0	18.7
Antipyrine	6.0	31.1	14.0
Atazanavir	100.0	110.8	110.0
Atenolol	2.8	2.5	6.6
Belinostat	19.0	13.2	12.7
Betaxolol	13.0	7.6	13.2
Bosentan hydrate	15.0	33.1	41.1
Bufuralol	20.6	10.0	19.5
Bupropion	6.0	15.5	19.7
Caffeine	17.0	15.8	5.7
Carvedilol	47.0	13.9	35.5
Cerivastatin	9.5	7.8	10.8
Chlorpheniramine	54.0	29.5	21.8
Chlorpromazine	45.0	38.2	50.5
Cimetidine	6.0	15.8	7.5
Coumarin	49.0	23.0	22.4
Cyclopropavir	7.0	9.0	5.8
Degrasyn	14.0	53.7	52.9
Desipramine	22.0	19.7	19.7
Diazepam	13.0	17.7	67.2
Diclofenac	131.0	11.7	14.5
Diltiazem	58.0	15.8	35.6
Diphenhydramine	39.0	19.2	12.9
Dofetilide	7.1	5.4	11.8
Furafylline	8.0	10.7	6.6
Furosemide	6.0	9.0	9.3
Gemfibrozil	29.0	8.3	22.3
Glipizide	29.0	24.8	13.0
Granisetron	6.0	8.2	9.1
Ibudilast	21.0	11.0	34.3
Ibuprofen	14.0	11.6	16.9

Imipramine	6.0	13.5	29.2
Irbesartan	14.0	16.0	20.1
Ketoprofen	13.0	11.7	11.2
Lorcainide	45.0	23.8	67.0
Mepazine	48.0	44.1	41.7
Mephenytoin	6.0	20.9	7.7
Metoprolol	6.0	5.8	9.7
Midazolam	>300.0	50.0	77.3
Nadolol	8.1	6.6	8.2
Naloxone	10.0	8.7	15.3
Naproxen	11.0	9.6	10.4
Ondansetron	37.0	27.5	13.7
Orphenadrine	6.0	20.8	14.8
Panobinostat	8.0	7.5	7.9
Paroxetine	18.0	16.2	20.8
Phenacetin	10.0	16.9	9.9
Pimozide	66.0	2.6	105.6
Pindolol	6.0	9.8	10.2
Pracinostat	13.0	14.6	11.3
Prazosin	8.0	15.6	12.2
Propafenone	20.0	11.5	20.0
Propranolol	30.0	9.2	14.1
Quinidine	37.0	16.4	18.6
Resminostat	8.0	10.6	6.7
Rifampicin	6.0	72.2	15.8
Risperidone	13.0	6.0	23.5
Semagacestat	6.0	23.3	9.3
Sildenafil	110.0	15.8	34.8
Spautin-1	40.0	36.1	35.1
Sulfaphenazole	29.0	16.5	15.3
Temozolomide	13.0	20.1	4.8
Testosterone	210.0	21.0	100.4
Ticlopidine	45.0	171.4	55.4
Tienilic Acid	41.0	14.0	15.9
Timolol	6.0	6.5	8.3
Tolbutamide	6.0	10.3	8.0
Tranylcypromine	6.0	24.1	16.8
Troglitazone	82.0	6.2	95.3
Warfarin	6.0	8.3	9.2
Venetoclax	23.0	2.4	45.8
Verapamil	200.0	79.8	94.9

CL_{int} = in vitro intrinsic clearance; HLM = human liver microsomes

Supplemental Table 3.

Measured Caco-2 P_{app} and predicted P_{app} from the in-house model for a set of reference compounds. Data is the mean of at least three independent experiments.

Compound	**Measured Caco-2 P_{app} (10^{-6} cm/s)**	**Predicted Caco-2 P_{app} (In-house model, 10^{-6} cm/s)**
Abexinostat	0.7	2.8
Aliskiren	0.2	1.2
Atazanavir	5.3	8.0
Atenolol	<1	1.0
Belinostat	5.9	11.8
Cyclopropavir	1.0	1.1
Degrasyn	4.9	19.7
Digoxin	1.0	1.1
Flupentixol	5.7	11.9
Ibudilast	43.0	23.7
Mepazine	16.0	14.8
Midazolam	42.0	18.6
Panobinostat	0.8	1.8
Phenacetin	47.0	20.6
Pimozide	12.0	12.4
Pracinostat	2.5	3.8
Propranolol	17.9	10.4
Resminostat	5.2	2.3
Rifampicin	12.0	3.7
Semagacestat	4.0	1.3
Sotrastaurin	3.3	4.1
Spautin-1	24.0	16.7
Thioridazine	18.0	13.5
Tracedinaline	8.4	13.2
Venetoclax	1.0	1.8
Z-Vrpr-Fmk (Malt Inhibitor)	1.0	0.9

P_{app} = apparent permeabiliy

Supplemental Table 4.

Analysis of variance for log transformed data shown in Supplemental Tables 2 and 3.

Assay		Coefficients	Standard error	t-ratio	P-value	Lower 95%	Upper 95%
Caco-2 (in house model versus measured values)	Intercept	0.260	0.076	3.42	0.002	0.103	0.418
	Slope	0.667	0.083	8.01	3.11E-08	0.495	0.839
HLM (global model versus measured values)	Intercept	0.825	0.108	7.63	7.03E-11	0.610	1.04
	Slope	0.280	0.081	3.45	0.001	0.118	0.442
HLM (in house model versus measured values)	Intercept	0.568	0.084	6.74	3.21E-09	0.400	0.737
	Slope	0.555	0.063	8.75	5.37E-13	0.428	0.681